

## New zirconium hydroxide

G. Y. GUO

*Department of Materials Science and Engineering, Shanghai Jiao Tong University, Shanghai 200030, People's Republic of China*  
E-mail: guo\_gongyi@hotmail.com

Y. L. CHEN

*College of Chemistry and Chemical Engineering, Shanghai University, Shanghai 200072, People's Republic of China*

The good properties of zirconia-based ceramics give them great potential for structural and functional applications. High-quality zirconia powder is vital for the successful development of advanced zirconia ceramics. Zirconium hydroxide, called hydrous zirconia, is an important precursor during the chemical preparation of zirconia powder. Formation of hydrous zirconia by forced hydrolysis under acidic conditions, homogeneous precipitation under alkaline conditions, and hydrolysis/condensation of alkoxide has been studied extensively both experimentally and theoretically [1–13]. However, only a few works have been devoted to the precipitation of hydrous zirconia under acidic conditions [14–16]. In addition, to the best of our knowledge, there have been no earlier reports on the structural characterization of the hydrous zirconia precipitated from aqueous zirconium oxychloride solution with aqueous ammonia under acidic conditions at ambient temperature. The present work attempts to supplement this knowledge of the relationship between the preparation conditions and properties of zirconium hydroxides by studying the precipitation of them at low pH values. This study will demonstrate that the zirconium hydroxides formed under acidic conditions can behave much differently from those precipitated under near-neutral or alkaline conditions. In addition, the zirconium hydroxides can, with a high yield, be produced by the controlled aqueous precipitation under acidic conditions, and result in an ultrafine, tetragonal-predominantly zirconia at a relatively high temperature (600 °C). It is, therefore, obvious that in comparison with the other processes, the present process offers distinct advantage in terms of the simplicity, ease of scale-up, low cost, and minimal environmental impact.

The zirconium oxychloride octahydrate was dissolved in deionized water so that the final concentration of zirconium was 38.76 g l<sup>-1</sup> (0.42 M). Five milliliters of the zirconyl chloride solution was added to 100 ml deionized water, and then concentrated aqueous ammonia were added dropwise to the solution with constant stirring until pH 4. The resultant precipitate was left for two days until the supernatant became nearly clear, filtered, washed with deionized water thoroughly, and dried at 70 °C for 56 h before characterization. The dried precipitate also called xerogel looks brown.

The zirconium in the zirconyl chloride solution, filtrate, and xerogel were assayed by inductively coupled plasma-atomic emission spectroscopy using a IRIS Advantage/1000 ICP-AES spectrophotometer (Thermo Jarrel Ash Corporation, USA). The determination of hydrogen and nitrogen in the xerogel was made by a Perkin Elmer Series II CHNS/O Analyzer 2400, USA. Fourier-transform infrared spectrum for the xerogel was recorded on a Bruker Equinox 55 spectrophotometer (Germany) in wavenumber 4000–400 cm<sup>-1</sup> range, with a resolution of 4 cm<sup>-1</sup> and a scan number of 25. The infrared spectrum of the xerogel was studied as powder dispersed in a KBr pellet. Fourier-transform laser Raman spectrum was taken from the xerogel, which was lightly compacted, at 3500–50 cm<sup>-1</sup> and a resolution of 4 cm<sup>-1</sup>, employing a Bruker Equinox 55 spectrophotometer, equipped with a near-infrared diode pumped Nd:YAG laser (1.064 μm). The laser power at the test samples was 400 mW.

The xerogel was examined by differential thermal analysis (DTA) and thermogravimetric analysis (TGA) with a thermal analyzer (Universal V2. 4F TA Instruments, USA). These experiments were conducted up to 800 °C with a heating rate of 10 °C min<sup>-1</sup> in air. A Bruker-AXS D8 advance diffractometer (Germany) was used to collect X-ray diffraction (XRD) data for the structural analysis of the xerogel and its pyrolysis products derived from its thermal treatment at different temperatures. The samples were scanned over a  $2\theta$  range of 20–90 °C at a scanspeed of 0.2 sec/step, with an increment 0.02 °/step using Cu K $\alpha$  radiation at 40 kV and 40 mA. The identification and quantification of monoclinic (M), tetragonal (T), and cubic (C) zirconia were accomplished by comparison of the XRD data to the Powder Diffraction File according to the relationships already used elsewhere [17, 18]. The crystallite sizes of the crystalline pyrolysis products were estimated by applying the well-known Scherrer equation to the half-height widths of reflections selected from the XRD patterns.

Even in strongly acidic solutions the hydrolysis of zirconium compounds will occur. Zirconium hydroxide precipitate can be produced by the hydrolysis of zirconium oxychloride in aqueous solution with an addition of ammonia at ca. pH2. The filtrates contain very little zirconium, suggesting that the precipitation

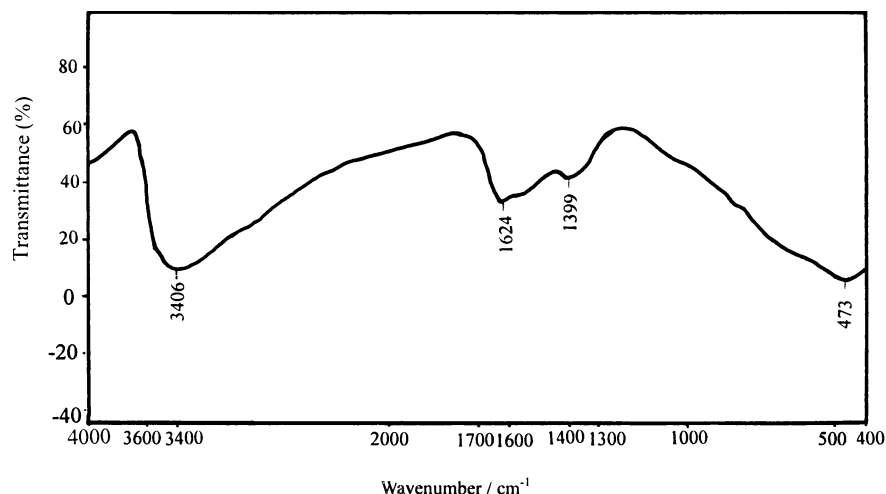


Figure 1 Infrared spectrum of the zirconium hydroxide xerogel obtained at pH 4.

of zirconium may be complete from the given concentration of aqueous zirconium oxychloride solution even when the final pH of the solution coexisting with the precipitate is as low as 4. The principal rationale for obtaining such a result is that the polynuclear positively charged species, e.g.,  $[\text{Zr}_4(\text{OH})_8(\text{H}_2\text{O})]_{16}^{8+}$ , of zirconium ion can exist even in very acidic solutions, and react with hydroxyl ions to form a precipitate [2, 5].

The infrared spectrum for the zirconium hydroxide precipitated at pH 4 is illustrated in Fig. 1. In the infrared spectrum the broad band centred upon  $3406\text{ cm}^{-1}$  may result from atmosphere moisture retained by the  $\text{KBr}$  pellet and from the OH groups in the zirconium hydroxide. The band at  $1624\text{ cm}^{-1}$  may be related to coordinated water due to the “scissor” bending mode of molecular water, and to an atmospheric constituent  $\text{CO}_2$  adsorbed on the xerogel, because  $\text{CO}_2$  is able to interact with terminal OH groups present on partially dehydrated xerogel surface, yielding bicarbonate-like species, whose O—C—O stretching bands are visible at  $\sim 1620\text{ cm}^{-1}$ . The band observed at  $1399\text{ cm}^{-1}$  may be attributed to bidentate carbonates formed by the “side-

on” coordination of atmospheric constituent  $\text{CO}_2$  on coordinatively unsaturated  $\text{O}^{2-}\text{-Zr}^{4+}$  pairs [19, 20]. There is no intense band around  $1000\text{ cm}^{-1}$ , characteristic of zirconyl group  $\text{Zr}=\text{O}$ , showing that the zirconium hydroxide is a polymer, in which the zirconium atoms are located between their oxygen bridges [1]. A broad band centred upon  $473\text{ cm}^{-1}$  is indicative of Zr—O bond vibration assignable to monoclinic and tetragonal zirconia [21–23], which will be confirmed by the Raman spectrum of the zirconium hydroxide precipitated at pH4.

The Raman spectrum of the zirconium hydroxide xerogels obtained at pH 4 is presented in Fig. 2. It may be noted from Fig. 2 that no Raman band is observed at  $490\text{ cm}^{-1}$  in the Raman spectrum of the zirconium hydroxide xerogels obtained at pH 4, indicating that the structure of the zirconium hydroxide is not related to cubic zirconia, since the Raman spectrum of cubic zirconia is distinguished by a single band with a frequency shift of  $490\text{ cm}^{-1}$  [5, 19, 24]. In the Raman spectrum (Fig. 2), the strong peaks at 153 and  $465\text{ cm}^{-1}$  can be assigned to tetragonal zirconia. The relatively strong peak at  $216\text{ cm}^{-1}$ , the broad peaks at 423 and  $1063\text{ cm}^{-1}$ , and

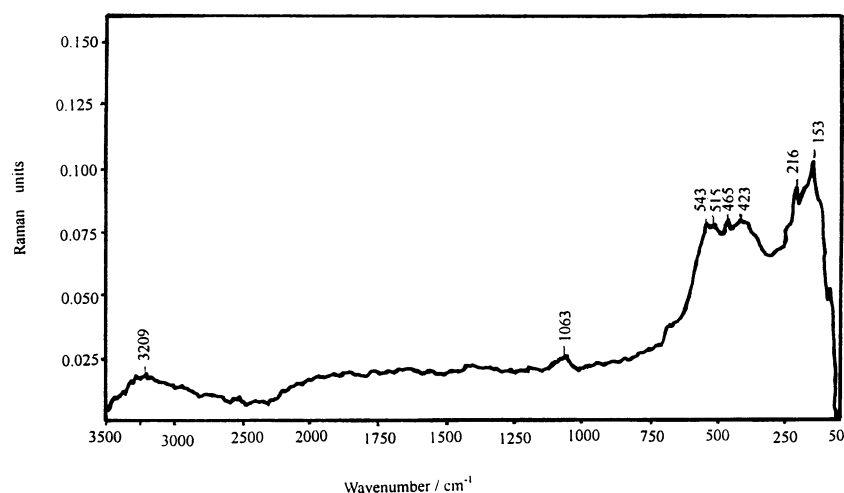


Figure 2 Raman spectrum of the zirconium hydroxide xerogel obtained at pH4.

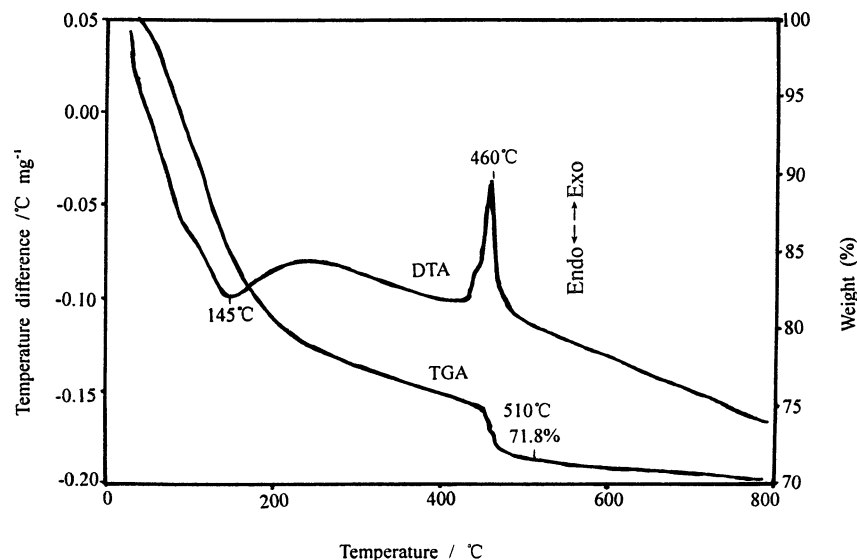


Figure 3 DTA and TGA curves of the zirconium hydroxide xerogel obtained at pH 4.

the weak peaks at 515 and 543  $\text{cm}^{-1}$  may be ascribed to monoclinic zirconia [18, 24–30]. These Raman features suggest that the structure of the amorphous zirconium hydroxide precipitated at pH4 is both tetragonal and monoclinic-like, supporting the above infrared assignment for the band at 473  $\text{cm}^{-1}$ .

Investigation of the thermal behavior of the zirconium hydroxides may be conducive in clarifying their composition and structure. It can be seen from the DTA curve (Fig. 3) that the zirconium hydroxide investigated shows two-step decomposition, an endothermic and an exothermic decomposition behaviors. The endothermic event occurs around 145 °C with a corresponding weight loss of 15%. Such a high-temperature dehydration indicates the water molecules present in the zirconium hydroxide investigated to be a coordinated water, which is supported by X-ray diffraction study. Fig. 4 shows that the zirconium hydroxide dehydrated at 150 °C remains amorphous to X-ray, suggesting the formation of no crystalline zirconia. After dehydration the zirconium hydroxide is progressively decomposed into amorphous zirconia due to dehydroxylation with increasing temperature, and a sharp exothermic peak

appears around 460 °C. The exothermic event is accompanied by an abrupt weight drop (3.2%), indicating that the decomposition is still being continued in the region of exothermic peak. The exothermic peak with weight change is assigned to a rapid release of bound hydroxyl groups at the higher temperature, resulting in fast formation and crystallization of the amorphous zirconia, yielding essentially 100% tetragonal phase, as evidenced by the X-ray diffraction pattern (Fig. 4). Even at a high calcination temperature, 600 °C, only a small fraction (18%) of the tetragonal phase will be transformed into monoclinic phase. The crystallite size of the tetragonal zirconia formed at 460 and 600 °C is 32 and 42 nm, respectively, suggesting that the crystallite size does not increase significantly as calcination temperature is raised, and the tetragonal phase can, therefore, be stabilized at a high temperature. In fact, it may be noted from the TGA curve that the loss of weight has ceased at 510 °C, indicating that the temperature seems to be sufficient for the calcination of the zirconium hydroxide into zirconia. At 510 °C the total weight has been reduced by 28.2%. In other words, the zirconia content in the zirconium hydroxide investigated

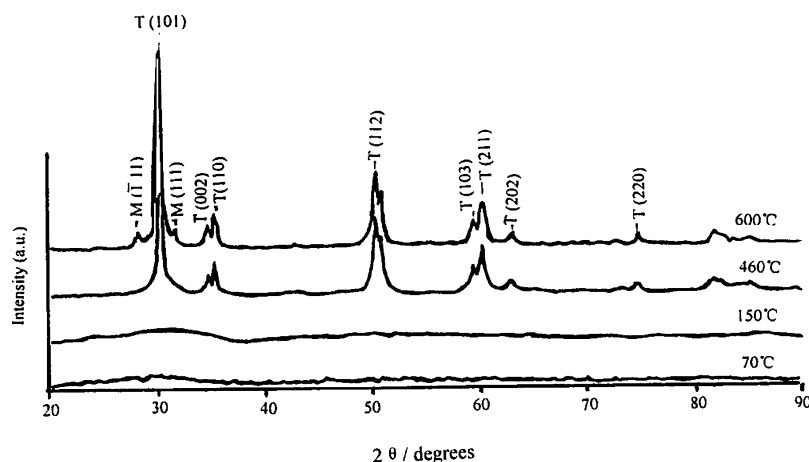


Figure 4 XRD patterns of the zirconium hydroxide xerogel (70 °C) obtained at pH 4 and its pyrolysis products at 150, 460, and 600 °C.

is 71.8%, i.e., zirconium is equal to 53.19%, which is consistent with the found value from the elemental analysis. The elemental analysis gave the following results (wt%): Zr, 53.17; H, 2.65; assuming the balance to be O, 44.18. The found values from the elemental analysis agrees well with those calculated for  $Zr_4O_3(OH)_{10} \cdot 6H_2O$ . A similar thermal behavior is also observed for the zirconium hydroxide precipitated at pH 3 (not shown). It is obvious that the thermal behavior of the zirconium hydroxide investigated is different from that of the existing zirconium hydroxides: [1, 11, 29, 31–34],  $\alpha$  [ $Zr_4(OH)_{16}$ ],  $\beta$  [ $Zr_4O_2(OH)_{12}$ ], and  $\gamma$  [ $Zr_4O_4(OH)_8$ , or  $[ZrO(OH)_2]$ ]. These zirconium hydroxides showed a single exothermic peak at around 420 °C and no endothermic peak in DTA curve; in the region of the exothermic peak hardly any weight loss was observed from TGA curve, and hence the exothermic peak was attributed to the transition from an amorphous to a tetragonal metastable phase of zirconia, i.e., a topotactic crystallization of tetragonal zirconia on nuclei present in the amorphous phase. When these hydroxides were heated in air, the losses of total weight were 22.6, 18 and 12.8%, respectively. We ascribe the difference between the thermal behavior of the zirconium hydroxide investigated and that of the well-established zirconium hydroxides to the different preparation pH values. The pH value was 3–4 (acidity) in this work and 9–10 (alkalinity) in the above literature. The preparation pH strongly affects the thermal behavior of zirconium hydroxides prepared at pH < 7. If pH is about 6, the zirconium hydroxide obtained exhibits a similar thermal behavior (not shown) to previous reports that conclude that hardly any weight loss in the region of the exothermic peak is observed from the TGA curve of zirconium hydroxide precipitated under alkaline conditions. Recently, the thermal behavior of the zirconium hydroxide investigated by us was also observed for hydrous zirconia prepared by hydrolytic condensation of zirconium n-propoxide in isopropanol at pH 1.5 or less [35]. The starting materials used were different from ours but the products obtained under acidic conditions had the similar thermal behavior.

The aqueous solution chemistry of zirconium has proved to be quite complicated. The tetrameric species  $[Zr_4(OH)_8(H_2O)_{16}]^{8+}$  is always present in both solid  $ZrOCl_2 \cdot 8H_2O$  and its aqueous solution due to the hydrolysis of zirconium (IV) in acidic conditions. The tetrameric species features a ring of four zirconium atoms, each linked to its neighbor by a pair of hydroxyl bridges. In addition, there are four water molecules bound to each zirconium atom to accomplish the eight-coordinate zirconium configuration. The polymerization for the zirconium species depends on the pH value of the liquid in contact with final hydroxide precipitate and on the presence or absence of complexing species, and hence may result in the products with various compositions and structures [3, 6, 36]. Polymerization will be more rapid with a higher pH value since more  $OH^-$  groups will be available to promote linking of corner/edges of the tetrameric units; more rapid linking/polymerization will inevitably result in more

defection sheet structures, whereas a lower pH will give rise to slower polymerization and a more ordered structure. These considerations are supported by the above Raman study. The bands in the Raman spectrum (Fig. 2) are relatively sharp, suggesting the presence of a better crystallinity in the zirconium hydroxide precipitated at pH 4. In conclusion, the zirconium hydroxides formed under acidic conditions have a composition and structure significantly different from those previously known, and hence behave much differently from the existing zirconium hydroxides precipitated under alkaline conditions. The DTA and TGA curves show that there is an abrupt weight drop for the former and hardly any weight loss for the latter in the region of the exothermic peak.

## References

1. L. M. ZAITSEV, *Russ. J. Inorg. Chem.* **11** (1966) 1684.
2. E. D. WHITNEY, *J. Amer. Ceram. Soc.* **53** (1970) 697.
3. M. A. BLESIA, A. J. G. MAROTO, S. I. PASSAGGIO, N. E. FIGLIOLIA and G. RIGORRI, *J. Mater. Sci.* **20** (1985) 4601.
4. S. L. JONES and C. J. NORMAN, *J. Amer. Ceram. Soc.* **71** (1988) C190.
5. R. SRINIVASAN, M. B. HARRIS, S. F. SIMPSON, R. J. DEANGELIS and B. H. DAVIS, *J. Mater. Res.* **3** (1988) 787.
6. G. T. MAMOTT, P. BARNES, S. E. TARLING, S. L. JONES and C. J. NORMAN, *J. Mater. Sci.* **26** (1991) 4054.
7. Y. T. MOON, H. K. PARK, D. K. KIM and C. H. KIN, *J. Amer. Ceram. Soc.* **78** (1995) 2690.
8. K. MATSUI and M. OHGAI, *ibid.* **80** (1997) 1949.
9. K. LEE, A. SATHYAGAL, P. W. CARR and A. V. McCORMICK, *ibid.* **82** (1999) 338.
10. M. Z.-C. HU, R. D. HUNT, E. A. PAYZANT and C. R. HUBBARD, *ibid.* **82** (1999) 2313.
11. N. SERGENT, J.-F. LAMONIER and A. ABOUKAIS, *Chem. Mater.* **12** (2000) 3830.
12. E. T. GARCIA, A. P. BARRANCO, C. V. RAMOS and G. A. FUENTES, *J. Mater. Res.* **16** (2001) 2209.
13. T. SATO, *J. Therm. Anal. Calorim.* **69** (2002) 255.
14. R. SRINIVASAN, C. R. HUBBARD, O. B. CAVIN and B. H. DAVIS, *Chem. Mater.* **5** (1993) 27.
15. J. L. TOSAN, B. DURAND, M. ROUBIN, F. BERTIN and H. LOISELEUR, *Eur. J. Solid State Inorg. Chem.* **30** (1993) 179.
16. G. ŠTEFANIC, S. MUSIC, B. GRZETA, S. POPOVIĆ and A. SEKULIĆ, *J. Solid Phys. Chem.* **59** (1998) 879.
17. G. Y. GUO, Z. F. NI and Y. L. CHEN, *J. Mater. Sci.* **26** (1991) 3511.
18. G. Y. GUO and Y. L. CHEN, *J. Amer. Ceram. Soc.* **75** (1992) 1294.
19. C. M. PHILLIPPI and K. S. MAZDIYASNI, *ibid.* **54** (1971) 254.
20. V. BOLIS, G. MAGNACCA, G. CERATTO and C. MORTERRA, *Thermochimica Acta* **379** (2001) 147.
21. A. A. M. ALI and M. I. ZAKI, *ibid.* **336** (1999) 17.
22. D. W. LIU, C. H. PERRY and R. P. INGEL, *J. Appl. Phys.* **64** (1988) 1413.
23. L. SHI, K. C. TIN and N. B. WONG, *J. Mater. Sci.* **34** (1999) 3367.
24. K. MATSUI and M. OHGAI, *J. Ceram. Soc. Jpn.* **106** (1998) 1232.
25. V. G. KERAMIDAS and W. B. WHITE, *J. Amer. Ceram. Soc.* **57** (1974) 22.
26. D. J. KIM and H. J. JUNG, *ibid.* **76** (1993) 2106.
27. F. LIU and J. YANG, *Phys. Rev. B* **55** (1997) 8847.
28. B. K. KIM and H. HAMAGUCHI, *Phys. Stat. Sol.* **b 203** (1997) 557.

29. S. XIE, E. IGLESIA and A. T. BELL, *Chem. Mater.* **12** (2000) 2442.
30. P. E. QUINTARD, P. BABÉRIIS and A. P. MIGORODSKY, *J. Amer. Ceram. Soc.* **85** (2002) 1745.
31. E. TANI, M. YOSHIMURA and S. SŌMIYA, *ibid.* **66** (1983) 11.
32. T. YAMAGUCHI, *Catal. Today* **20** (1994) 199.
33. J. MATTA, J. F. LAMONIER, A. A. EDMOND, E. A. ZHILINSKAYA and A. ABOUKAÏS, *PCCP* **1** (1999) 4975.
34. E. TORRES-GARCIA, A. PELÁIZ-BARRANCO, C. VÁZQUEZ-RAMOS and G. A. FUENTES, *J. Mater. Res.* **16** (2001) 2209.
35. G. ŠTEFANIĆ, I. I. ŠTEFACĆ and S. MUSIČ, *Mater. Chem. Phys.* **65** (2000) 197.
36. A. CLEARFIELD, *J. Mater. Res.* **5** (1990) 161.

*Received 25 June  
and accepted 23 December 2003*